DOI 10.52209/2706-977X_2024_4_51 **IRSTI 29.19.16** **UDC 53.02**

Strength Calculation of Variable Bending Rigidity Rods in the Presence of Initial Cambers along Their Axes

Akhmediyev S.K., Filippova T.S., Oryntayeva G.Zh., Tazhenova G.D.*
Abylkas Saginov Karaganda Technical University, Karaganda, Kazakhstan
*corresponding author

Abstract. The paper studies the stress-strain state of a rod with variable bending rigidity, compressed by an axial concentrated force in the presence of initial deflections along its axis. The initial differential equation of longitudinal bending is solved by the numerical finite difference method with the number of divisions along the axis equal to eight. Two problems are solved simultaneously: bending strength and stability under central compression. The calculated deflection diagrams are given depending on the change in the axial load value, taken as a fraction of the critical force, as well as depending on the conditions of fixing the ends of the rod. The results of the study are the formation of 7th order resolution matrices for the numerical calculation of longitudinal-transverse bending of the rod. Critical forces for various boundary conditions at the ends of the rod, and the values of the resulting deflections are determined.

Keywords: rod, bending, stability, finite difference method, deflection.

Introduction

The rod elements of various designs of transport systems, mechanisms, mobile transport [6], buildings, structures, as well as aircraft and shipbuilding structures have manufacturing and operating defects in the form of initial cambers along their longitudinal axes (transverse to the axes of linear deformations).

In these cases, the structures (technical systems) under consideration operate under conditions of the complex stress state (with flat transverse bending).

Load-bearing elements of mechanical engineering structures are in the same conditions, which require strength analysis within the limits of long-term operation [1-2].

In the process of their designing, it is necessary to identify the stress-strain state (determining linear and angular deformations, displacements, internal axial forces and bending moments in the corresponding bending plane) based on the values of which cross sections are selected according to the conditions of strength and rigidity, ensuring safe (reliable) operation of the considered systems.

For example, the study of the stress-strain state, longitudinal vibrations of rods of variable cross-section are considered in articles [7, 8, 11, 12]. In addition, impact [9, 10, 13], combined loading, dynamic stability [14, 15] of rods under various boundary conditions are often studied.

The purpose of the article is to study the stress-strain state of a complex rod system with a variable cross-sectional thickness along the length in the presence of constructive and acquired during operation " cambers " based on the numerical finite difference method taking into account longitudinal transverse bending with the determination of the resulting deflections and the value of the critical forces of central compression.

Let us consider a rod of variable bending rigidity (variable thickness) compressed by the “P” force, taking into account the given initial cambers $f_0(x)$ along the longitudinal axis with random boundary conditions at its ends (Figure 1). Here: y=y(x) is a function of the desired cambers along the longitudinal axis of the rod, $f_0 = f_0(x)$ is a known function of initial cambers (linear displacements along the “y” axis); $J_i = J(x)$is a variable axial moment of inertia of the cross section.

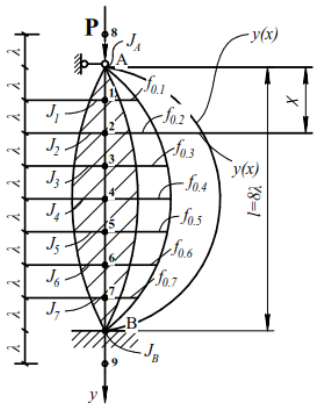

Fig. 1 – Design diagram of the rod under study

1. Methods and solutions

The initial differential equation describing the mechanical operation of the structure under study (Figure 1) has the form [1, 2, 5]:

$$(EJY^{IV} + EJ^{II}Y^{II}) + 2EJ^{I}Y^{III} + PY^{II} = Pf_0^{II}(x). \quad (1)$$

Both parts of equation (1) are divided by the value EJ_0 (the conditional (scale) bending rigidity of the rod], and the notation is introduced in the form of $(K = \frac{P}{EJ_0})$ as the axial load parameter.

Then, taking into account "***K"***, instead of equation (1), there is obtained the following equation:

$$\frac{EJ}{EJ_0}Y^{IV} + \frac{EJ^{II}}{EJ_0}Y^{II} + \frac{2EJ^{I}}{EJ_0}Y^{III} + KY^{II} = -Kf_0^{(I)}(x). \quad (2)$$

Equation (2) is implemented using the finite difference method (FDM) with a linear grid with a density equal to the "n" value; a fragment of such a grid is shown in Figure 2.

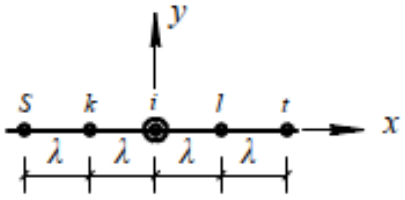

Fig. 2 – A fragment of a regular "linear grid"

Let's write equation (2) in general form for the *i*-th grid node (Figure 2), using the FDM parameters known from [3÷5], taking this into account:

$$K^* = k\lambda^2 = \frac{P}{EJ_0}\lambda^2 \quad (3)$$

K^* is the grid parameter of the axial load.

$$\frac{\alpha_i(y_t - 4y_l + 6y_i - 4y_k + y_s)}{\lambda^4} + \frac{(\alpha_l - 2\alpha_i + \alpha_k)(y_l - 2y_i + y_k)}{\lambda^4} +$$
$$+\frac{0{,}5}{\lambda^4}(\alpha_l - \lambda_k)[y_t - 2(y_l - y_k) - y_s] + \frac{k^*}{\lambda^4}(y_l - 2y_i + y_k) =$$
$$= -\mathrm{k}^*(\mathrm{f}_{0,\mathrm{l}} - 2\mathrm{f}_{0,\mathrm{i}} + \mathrm{f}_{0,\mathrm{k}}), \text{ or}$$
$$y_t[\alpha_i + 0{,}5\,(\alpha_l - \alpha_k)] + y_l[-4\alpha_i + (\alpha_l - 2\alpha_i + \alpha_k) - (\alpha_l - \alpha_k) + k^*] + \; + y_i[6\alpha_i - 2(\alpha_l - 2\alpha_i + \alpha_k) - 2k^*] +$$
$$y_k[-4\alpha_i + (\alpha_l - 2\alpha_i + \alpha_k) + +(\alpha_l - \alpha_k) + k^*] + y_s[\alpha_i - 0{,}5\,(\alpha_l - \alpha_k)] = -\mathrm{k}^*(\mathrm{f}_{0,\mathrm{l}} - 2\mathrm{f}_{0,\mathrm{i}} + \mathrm{f}_{0,\mathrm{k}})$$

Then, after reducing similar terms, there is obtained the following:

$$y_t[\alpha_i + 0{,}5\,(\alpha_l - \alpha_k)] + y_l(-6\alpha_i + 2\alpha_k + k^*) + y_i[10\alpha_i - 2(\alpha_l + \alpha_k) - 2k^*] + y_k(-6\alpha_i + 2\alpha_l + k^*) +$$
$$y_s[\alpha_i - 0{,}5\,(\alpha_l - \alpha_k)] = -\mathrm{k}^*(\mathrm{f}_{0,\mathrm{l}} - 2\mathrm{f}_{0,\mathrm{i}} + \mathrm{f}_{0,\mathrm{k}})\,; \quad (4)$$

Let's write expression (4) in the reduced form:

$$y_t \cdot \varphi_t + y_l \cdot \varphi_l + y_i \cdot \varphi_i + y_k \cdot \varphi_k + y_s \cdot \varphi_s = -\gamma k^*(\mathrm{f}_{0,\mathrm{l}} - 2\mathrm{f}_{0,\mathrm{i}} + \mathrm{f}_{0,\mathrm{k}}) \quad (5)$$

where

$$y_t = \alpha_i + 0{,}5\,(\alpha_l - \alpha_k)\,;\ \varphi_l = -6\alpha_i + 2\alpha_k + k^*\gamma\,;$$
$$\varphi_i = 10\alpha_i - 2(\alpha_l + \alpha_k) - 2k^*\gamma\,;\ \varphi_k = -6\alpha_i + 2\alpha_l + k^*\gamma\,; \quad (6)$$
$$\varphi_s = \alpha_i - 0{,}5\,(\alpha_l - \alpha_k)\ .$$

Let's divide the length of a given rod "l" into 8 equal parts (the grid density n=8) and number the calculated nodes of the linear grid m=1, 2..., 7 (Figure 1).

Let's write finite-difference equations according to formula (5) for the design nodes, excluding the deflections of the contour nodes 8, 9 using the boundary conditions at the ends of the rod, i.e.

$$y_{8=}\beta_1 y_1;\ y_{9=}\beta_2 y_7, \quad (7)$$

where (β_1, β_2)=+1 with the fixed end of the rod,

(β_1, β_2)=-1 with the hinged end.

1) Node "1" ($i = 1$):

$\beta_1 \cdot y_1[\alpha_1 + 0{,}5(\alpha_A - \alpha_2)] + y_1[10\alpha_1 - 2(\alpha_2 + \alpha_A) - 2k^* \cdot \gamma] + +y_2(-6\alpha_1 + 2\alpha_A + k^* \cdot \gamma) + y_3[\alpha_1 - 0{,}5(\alpha_A - \alpha_2)] = -\gamma \cdot k^*(f_{0,2} - 2f_{0,1})$,

or

$$y_1[-1{,}5\alpha_A + (10 + \beta_1)\alpha_1 - 2{,}5\alpha_2 - 2k^* \cdot \gamma] + y_2(2\alpha_A - 6\alpha_1 + k^* \cdot \gamma) + +y_3(-0{,}5\alpha_A + \alpha_1 + 0{,}5\alpha_2) = -\gamma k^*(f_{0,2} - 2f_{0,1}) \quad (8)$$

2) Node "2" ($i = 2$)

$y_1(-6\alpha_2 + 2\alpha_3 + k^* \cdot \gamma) + y_2[10\alpha_2 - 2(\alpha_A + \alpha_3) - 2k^* \cdot \gamma] + y_3(-6\alpha_2 + +2\alpha_1 + k^* \cdot \gamma) + y_4[\alpha_2 - 0{,}5(\alpha_1 - \alpha_3)] = -k^* \cdot \gamma(f_{0,1} - 2f_{0,2} + f_{0,3})$

or

$y_1(-6\alpha_2 + 2\alpha_3 + k^* \cdot \gamma) + y_2(-2\alpha_A + 10\alpha_2 - 2\alpha_3 - 2k^* \cdot \gamma) + y_3(2\alpha_1 - -6\alpha_2 + k^* \cdot \gamma) + y_4(-0{,}5\alpha_1 + \alpha_2 + 0{,}5\alpha_3) = -k^* \cdot \gamma(f_{0,1} - 2f_{0,2} + f_{0,3})$

3) Node "3" ($i = 3$)

$$y_1[\alpha_3 + 0{,}5(\alpha_2 - \alpha_4)] + y_2(-6\alpha_3 + 2\alpha_4 + k^* \cdot \gamma) + y_3[10\alpha_3 - 2(\alpha_2 + \alpha_4) - 2k^* \cdot \gamma] +$$

$$+y_4(-6\alpha_3 + 2\alpha_2 + k^* \cdot \gamma) + y_5[\alpha_3 - 0{,}5(\alpha_2 - \alpha_4)] = -k^* \cdot \gamma(f_{0,2} - -2f_{0,3} + f_{0,4}) \quad (9)$$

or

$y_1(0{,}5\alpha_2 + \alpha_3 - 0{,}5\alpha_4) + y_2(-6\alpha_3 + 2\alpha_4 + k^* \cdot \gamma) + y_3(-2\alpha_2 + 10\alpha_3 - 2\alpha_4 - 2k^* \cdot \gamma) + y_4(2\alpha_2 - 6\alpha_3 + k^* \cdot \gamma) + y_5(-0{,}5\alpha_2 + \alpha_3 + 0{,}5\alpha_4) = -k^* \cdot \gamma$

$$(f_{0,2} - 2f_{0,3} + f_{0,4}) \quad (10)$$

4) Node "4" ($i = 4$)

$y_2[\alpha_4 + 0{,}5(\alpha_3 - \alpha_5)] + y_3(-6\alpha_4 + 2\alpha_5 + k^* \cdot \gamma) + y_4[10\alpha_4 - 2(\alpha_3 + \alpha_5) - 2k^* \cdot \gamma] + y_5(-6\alpha_4 + 2\alpha_3 + k^* \cdot \gamma) + y_6[\alpha_4 - 0{,}5(\alpha_3 - \alpha_5)] = -k^* \cdot \gamma(f_{0,3} - 2f_{0,4} + f_{0,5})$,

or

$$y_2(0{,}5\alpha_3 + \alpha_4 - 0{,}5\alpha_5) + y_3(-6\alpha_4 + 2\alpha_5 + k^* \cdot \gamma) + y_4(-2\alpha_3 + 10\alpha_4 - 2\alpha_5 - 2k^* \cdot \gamma) +$$

$$+y_5(2\alpha_3 - 6\alpha_4 + k^* \cdot \gamma) + y_6(-0{,}5\alpha_3 + \alpha_4 + 0{,}5\alpha_5) = -k^* \cdot \gamma(f_{0,3} - 2f_{0,4} + f_{0,5}) \quad (11)$$

5) Node "5" ($i = 5$)

$y_3[\alpha_5 + 0{,}5(\alpha_4 - \alpha_6)] + y_4(-6\alpha_5 + 2\alpha_6 + k^* \cdot \gamma) + y_5[10\alpha_5 - 2(\alpha_4 + \alpha_6) - 2k^* \cdot \gamma] + y_6(-6\alpha_5 + 2\alpha_4 + k^* \cdot \gamma) + y_7[\alpha_5 - 0{,}5(\alpha_4 - \alpha_6)] = -k^* \cdot \gamma(f_{0,4} - -2f_{0,5} + f_{0,6})$,

or

$$y_3(0{,}5\alpha_4 + \alpha_5 - 0{,}5\alpha_6) + y_4(-6\alpha_5 + 2\alpha_6 + k^* \cdot \gamma) + y_5(-2\alpha_4 + 10\alpha_5 - 2\alpha_6 - 2k^* \cdot \gamma) +$$

$$+y_6(2\alpha_4 - 6\alpha_5 + k^* \cdot \gamma) + y_7(-0{,}5\alpha_4 + \alpha_5 + 0{,}5\alpha_6) = -k^* \cdot \gamma(f_{0,4} - 2f_{0,5} + f_{0,6}) \quad (12)$$

6) Node "6" ($i = 6$)

$y_4[\alpha_6 + 0{,}5(\alpha_5 - \alpha_7)] + y_5(-6\alpha_6 + 2\alpha_7 + k^* \cdot \gamma) + y_6[10\alpha_6 - 2(\alpha_5 + \alpha_7) - 2k^* \cdot \gamma] + y_7(-6\alpha_6 + 2\alpha_5 + k^* \cdot \gamma) = -k^* \cdot \gamma(f_{0,5} - 2f_{0,6} + f_{0,7})$,

or

$$y_4(0{,}5\alpha_5 + \alpha_6 - 0{,}5\alpha_7) + y_5(-6\alpha_6 + 2\alpha_7 + k^* \cdot \gamma) + y_6(-2\alpha_5 + 10\alpha_6 - 2\alpha_7 - 2k^* \cdot \gamma) + +y_7(2\alpha_5 - 6\alpha_6 + k^* \cdot \gamma) = -k^* \cdot \gamma(f_{0,5} - 2f_{0,6} + f_{0,7}) \quad (13)$$

7) Node "7" ($i = 7$)

$y_5[\alpha_7 + 0{,}5(\alpha_6 - \alpha_\beta)] + y_6(-6\alpha_7 + 2\alpha_\beta + k^* \cdot \gamma) + y_7[10\alpha_7 - 2(\alpha_6 + \alpha_\beta) - 2k^* \cdot \gamma] + \beta_2 y_7[\alpha_7 - 0{,}5(\alpha_6 - \alpha_\beta)] = k^* \gamma(f_{0,6} - 2f_{0,7})$,

or

$$y_5(-0{,}5\alpha_\beta + 0{,}5\alpha_6 + \alpha_7) + y_6(2\alpha_\beta - 6\alpha_7 + k^* \cdot \gamma) +$$
$$+y_7[\alpha_\beta(-2 + 0{,}5\beta_2) - \alpha_6(2 + 0{,}5\beta_2) + \alpha_7(10 + \beta_2) - 2k^* \cdot \gamma] = -k^* \cdot \gamma(f_{0,6} - 2f_{0,7}). \quad (14)$$

Let's reduce equations (8-14) into a single system of linear algebraic equations (SLAE) of the 7th order (Table 1). By changing the initial parameters of a given rod (Figure 1), it is possible to solve various problems regarding the strength of compressed rods with different boundary conditions with variable bending rigidity in the presence of initial cambers ($f_{0,x}$).

After solving the 7th order SLAE (the rigidity structure is shown in Table 1), their transverse displacements (deflections) along the axes of the rods at the calculated grid nodes (Figure 1) are determined: $y_1, y_2, \dots, y_7$. Based on the values of these deflections, the values of bending moments at the *i*-th grid nodes are determined (according to the template in Figure 2):

$$M_{x_i} = -EJ_i \frac{d^2 y_i}{dx^2} = -\frac{64}{l^2}(y_k - 2y_i + y_l). \quad (15)$$

In Table 1, variable alphabetic symbols (Figure 1) mean the following:

$(\alpha_A, \alpha_B, \alpha_1 \div \alpha_7)$ is the variability of the structure thickness along the length of the rod in design nodes A, 1, 2, ...7, B according to the law of their changing (in particular, it can be accepted according to the law of a square parabola);
$(\alpha_A, \alpha_B, \alpha_1 \div \alpha_7)$ are the value of the initial losses at nodes 1, 2, …, 7 (considered known before the start of calculations);
β_1, β_2 are coefficients for specifying boundary conditions at the ends of the rod (nodes A, B); they are taken equal to "+1" when supports "A" or "B" are rigidly fixed; "-1" when they are hinged (Table 1).

Table 1. Resolving finite-difference equations

No.	y_1	y_2	y_3	y_4	y_5	y_6	y_7	Right part
1	$(0{,}5\beta_1 - 2)\alpha_A + (10 + \beta_1)\alpha_1 - (0{,}5\beta_1 + 2)\alpha_2 + 2k^* \cdot \gamma$	$2\alpha_A - 6\alpha_1 + k^*\gamma$	$-0{,}5\alpha_A + \alpha_1 + 0{,}5\alpha_2$					$-\gamma_1 k^*(f_{0,2} - 2f_{0,1})$
2	$-6\alpha_2 + 2\alpha_3 + k^*\gamma$	$-2\alpha_A + 10\alpha_2 - 2\alpha_3 - 2k^*\gamma$	$-2\alpha_1 - 6\alpha_2 + k^*\gamma$	$-0{,}5\alpha_1 \alpha_2 + 0{,}5\alpha_3$				$-\gamma_1 k^*(f_{0,1} - 2f_{0,2} + f_{0,3})$
3	$0{,}5\alpha_2 + \alpha_3 - 0{,}5\alpha_4$	$-6\alpha_3 + 2\alpha_4 + k^*\gamma$	$-2\alpha_2 + 10\alpha_3 - 2\alpha_4 - 2k^*\gamma$	$2\alpha_2 - 6\alpha_3 + k^*\gamma$	$-0{,}5\alpha_2 + \alpha_3 + 0{,}5\alpha_4$			$-\gamma_1 k^*(f_{0,2} - 2f_{0,3} + f_{0,4})$
4		$0{,}5\alpha_3 + \alpha_4 - 0{,}5\alpha_5$	$-6\alpha_4 + 2\alpha_5 + k^*\gamma$	$-2\alpha_3 + 10\alpha_4 - 2\alpha_5 - 2k^*\gamma$	$2\alpha_3 - 6\alpha_4 + k^*\gamma$	$-0{,}5\alpha_3 + \alpha_4 + 0{,}5\alpha_5$		$-\gamma_1 k^*(f_{0,3} - 2f_{0,4} + f_{0,5})$
5			$0{,}5\alpha_4 + \alpha_5 - 0{,}5\alpha_6$	$-6\alpha_5 + 2\alpha_6 + k^*\gamma$	$-2\alpha_4 + 10\alpha_5 - 2\alpha_6 - 2k^*\gamma$	$2\alpha_4 - 6\alpha_5 + k^*\gamma$	$0{,}5\alpha_4 + \alpha_5 + 0{,}5\alpha_6$	$-\gamma_1 k^*(f_{0,4} - 2f_{0,5} + f_{0,6})$
6				$0{,}5\alpha_5 + \alpha_6 - 0{,}5\alpha_7$	$-6\alpha_6 + 2\alpha_7 + k^*\gamma$	$-2\alpha_5 + 10\alpha_6 - 2\alpha_7 - 2k^*\gamma$	$2\alpha_5 - 6\alpha_6 + k^*\gamma$	$-\gamma_1 k^*(f_{0,5} - 2f_{0,6} + f_{0,7})$
7					$0{,}5\alpha_6 + \alpha_7 - 0{,}5\alpha_8$	$2\alpha_6 - 6\alpha_7 + k^*\gamma$	$\alpha_6(0{,}5\beta_2 - 2) + (10 + \beta_2)\alpha_7 - \alpha_6(0{,}5\beta_2 + 2) - 2k^* \cdot \gamma$	$-\gamma_1 k^*(f_{0,6} - 2f_{0,2})$

The calculation using the proposed numerical model is carried out in the form of the following two sequential algorithms:

1. Calculating stability of variable thickness rods without initial cambers $(f_1, = f_2 = \cdots = f_7 = 0{,}0)$ with various boundary conditions, under which the parameters of the critical force k_{min} are determined; the critical force in these cases is determined from formula (3):

$$P_{\text{кр}} = 64K_{min}\left(\frac{EJ_0}{l^2}\right). \quad (16)$$

2. Taking into account the obtained values of "k_{min}", the calculations are performed for rods of variable bending rigidity (thickness) under various boundary conditions (a combination of hinged or rigid supports "A" and "B") in the absence and presence of initial cambers $f_1, f_2, \dots, f_7$; these calculations examine the strength of compressed-bent rods when varying the ratios (P/Pcr) that are specified by the coefficients γ, γ_1 varying in the range from 0.1 to 0.9 with a step of 0.1, while linear displacements along the axes of the rods are determined (deflections $y_1, y_2, \dots, y_7$), the bending moments (according to formula 15).

Then, based on the data in Table 1, the following results were obtained:

1) The calculation of a compressed rod for stability:

a) a rod of variable thickness that changes according to the law of a sinusoid: $t=y_0 \sin\left(\frac{\pi x}{l}\right)$ with three options of boundary conditions (Figure 1):

- option "I" - hinges on supports "A" and "B";
- option "II" - rigid sealing on supports "A" and "B";
- option "III" - hinge in support "A", seal in support "B"; in this case, the thickness coefficients at the grid nodes (Figure 1) $\alpha_A = \alpha_B = 0.31;\ \alpha_1 = \alpha_7 = 0.588; \alpha_2 = \alpha_6 = 0.81; \alpha_3 = \alpha_5 = 0.952;\ \alpha_4 = 1.0$.

The results are the values of the critical load parameter "*K*" (in formula 2) (Table 2).

Table 2. "*K*" values depending on the boundary conditions at the variable thickness rod ends

Option of boundary conditions	I	II	III
"*K*" values (variable thickness rod)	0.078	0.135	0.106
"*K*" values (constant thickness rod)	0.152	0.586	0.306

According to Table 2, the graphs of changing the critical load parameter "*K*" are plotted (Figure 3).

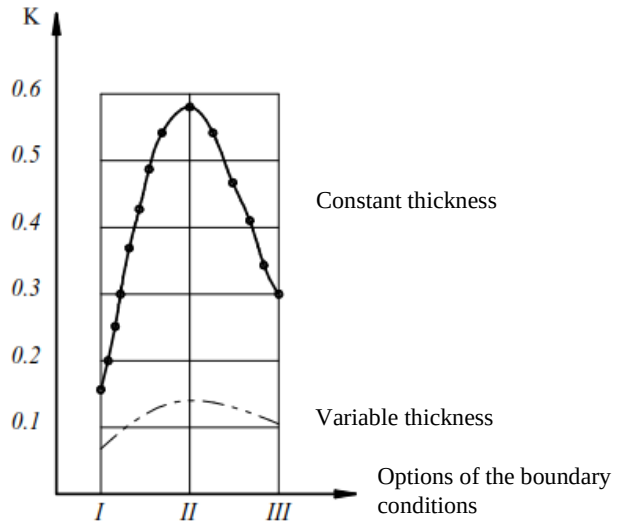

Fig. 3 – "K" dependence on the boundary conditions

2. Calculation of compressed rod strength

- rod thickness is constant ($\alpha_i = const$ =1.0);
- the initial losses, specified according to the sinusoid law, change:

f(x) = $f_0 \sin(\frac{\pi x}{l})$ ($f_0 = 1$ cm);

- initial load step:

$P_i = \gamma \cdot K_i$ (K_i→according to Table 2; γ=0.1;0.2;0.4;0.6;0.8;0.9).

Table 3 shows the values of deflections y_i (i ==1, 2, 3, ... 7) for three options of boundary conditions: I, II, III (rod of constant thickness). Figure 4 shows the graphical dependences of the deflections y_i (i =1.2,...7) in the design nodes of rods of constant thickness at γ=0.1;0.2;0.4;0.6;0.8 ;0.9 for three variants of boundary conditions I, II, III (according to Table 3).

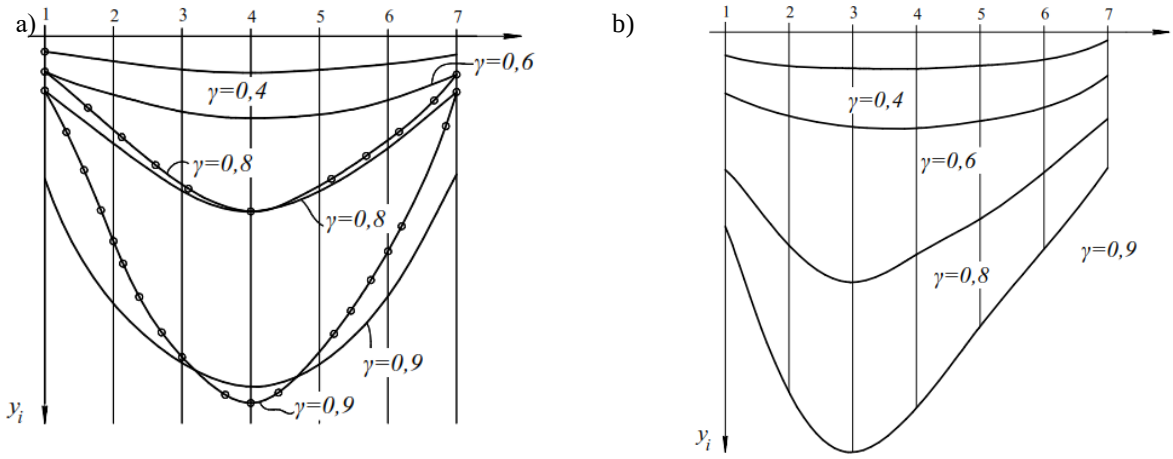

Fig. 4 – Diagrams of deflections of compressed rods of constant thickness in the presence of initial deflections for three variants of boundary conditions:
a) options I, II; b) option III

Table 3. Deflection values in the constant thickness rod

γ value	y_i value																				
	I							II								III					
	y_1	y_2	y_3	y_4	y_5	y_6	y_7	y_1	y_2	y_3	y_4	y_5	y_6	y_7	y_1	y_2	y_3	y_4	y_5	y_6	y_7
0,1	0.034	0.064	0.085	0.093	0.085	0.064	0.034	0.016	0.049	0.081	0.097	0.081	0.049	0.016	0.035	0.065	0.083	0.085	0.066	0.038	0.012
0,2	0.077	0.143	0.190	0.209	0.190	0.143	0.077	0.036	0.109	0.183	0.219	0.183	0.109	0.036	0.080	0.146	0.186	0.190	0.148	0.085	0.027
0,4	0.205	0.383	0.507	0.554	0.507	0.983	0.205	0.093	0.290	0.487	0.580	0.487	0.290	0.093	0.217	0.394	0.496	0.498	0.385	0.219	0.069
0,6	0.465	0.865	1.14	1.242	1.14	0.865	0.465	0.202	0.649	1.095	1.297	1.095	0.649	0.202	0.500	0.899	1.114	1.096	0.839	0.473	0.145
0,8	1.248	2.314	3.037	3.298	3.037	2.314	1.248	0.520	1.719	2.918	3.438	2.918	1.719	0.520	1.373	2.438	2.964	2.851	2.154	1.195	0.358
0.9	2.818	5.215	6.830	7.406	6.830	5.215	2.818	1.148	3.845	6.561	7.709	6.561	3.854	1.148	3.139	5.539	6.661	6.321	4.736	2.603	0.769

Conclusions

1. In this work, a study was carried out of the stress-strain state (SSS) of rods of variable bending stiffness (variable thickness along the length of the rod) with various boundary conditions [a combination of hinge and pinching at the ends of the rods] in the absence and presence of initial cambers identified in the course of manufacturing or operation process.

2. The resulting calculation method was chosen to be the numerical finite difference method (FDM) using a regular linear grid of density n=8; The study is based on a double calculation algorithm: calculations of rods for stability in the absence of initial failures; strength calculations in the presence of initial failures of compressed-bent rods under the action of axial load ($^{P}/_{P_{cr}}$) in the 0.1; 0.2; …; 0.9 ratios.

3. In the stability calculation algorithm, the critical force $P_{кр}$ is determined; strength of linear displacements and bending moments at design nodes 1, 2, …, 7 (Figure 1).

4. A number of research tasks were completed:

a) stability of compressed rods of constant and variable thickness along their length (Table 2, Figure 3);

b) strength of compressed rods of constant thickness in the presence of initial cambers varying along the length of the rod according to the sinusoidal law with increasing the axial load from 10 to 90% of the value of the corresponding critical force (Table 3, Figure 4);

5. When analyzing the results of the above studies, the following was established:

a) the value of the critical forces for all three considered options of boundary conditions I, II, III for variable thickness rods is smaller than that for the same rods of constant thickness (Figure 3);

b) deflections in the calculated grid nodes y_i (i=1, 2, …, 7) in the presence of initial cambers, with increasing the value of the corresponding load ($P_i = \gamma_i . P_{кр}$) also increase monotonically; at the same time, for rods with hinged supports at the "A" and "B" nodes, option I (Figure 1), the absolute values of deflections are greater than for the other options of boundary conditions II, III (Figure 4, a, b).

6. The theoretical principles and applied results presented in this work can be used in studying the mechanics of rod systems, as well as in designing real structures used in various branches of technology.

References

[1] Kisselev V.A. Structural mechanics: Special course. Dynamics and stability of structures. M.: Stroyizdat, 1980. - 676 p.

[2] Handbook for designers of industrial and public buildings and structures. Calculation and theory, book 2; edited by A.A. Umansky. - M.: Stroyizdat, 1972. - 600 p.

[3] Akmehdiyev S.K., et al. Analytical numerical methods for calculating machine-building and transport structures. - Karaganda: KTU Publishing House, 2016. - 158 p.

[4] Varvak P.M., Varvak L.P. The grid method in problems of calculating building structures. - M.: Stroizdat, 1977. - 160 p.
[5] Bakirov Zh.B., Zhadrassinov N.T., Akhmediyev S.K. Computational mechanics: Tutorial. Karaganda: KTU Publishing House, 2004. 102 p.
[6] Akhmediyev S.K., Filippova T.S., Tazhenova G.D., Mikhailov V.F. Free and Forced Vibrations of the Carrier Beam of the Vehicle Chassis //Material and mechanical engineering technology. Karaganda: KSTU, 2023. Vol. 4, No. 4. P. 32-42.
[7] Tsarenko S., Ulitin G. /Investigation of strained deformed state of variable stiffness rod// SpringerPlus, 2014. Vol 3. P. 367 DOI: 10.1186/2193-1801-3-367
[8] Ulitin G., Tsarenko S. Longitudinal Vibrations of Elastic Rods of Variable Cross-Section //International Applied Mechanics, 2015. Vol. 51, Issue 1, P. 102 – 107.
[9] Bityurin A. A. //Calculation of the critical velocity of a stepwise rod system under a longitudinal impact// Journal of Applied Mechanics and Technical Physics. 2011. Vol. 52, Issue 4, P. 530 – 535.
[10] Schwarz C., Fischer F. D., Werner E., Dirschmid H. J. //Impact of an elastic rod on a deformable barrier: Analytical and numerical investigations on models of a valve and a rod-shaped stamping tool// Archive of Applied Mechanics. 2009. Vol. 80, P. 3–24.
[11] Ulitin G. //The longitudinal vibrations of an elastic rod simulating a drilling rig// International Applied Mechanics. 2000. Vol. 36, Issue 10, P. 1380 – 1384.
[12] Werner E. A., Fischer F. D. //The stress state in a moving rod suddenly elastically fixed at its trailing end// 1995. Acta Mechanica. Vol. 111, Issue 3-4, P. 171 – 179.
[13] Xing Yufeng, Qiao Yuansong, Zhu Dechao, Sun Guojiang //Elastic impact on finite Timoshenko beam// Acta Mechanica Sinica. 2002. Vol. 18, P. 252–263.
[14] Cheremnykh S. Stability of the steel rod under combined loading //AIP Conference Proceedings. 2023. Vol. 2526, Issue 15.
[15] Belyaev A. K., Ilin D. N. and Morozov N. F. //Stability of transverse vibration of rod under longitudinal step-wise loading// Journal of Physics: Conference Series. Vol. 451. DOI 10.1088/1742-6596/451/1/012023

Information of the authors

Akhmediev Serik Kabultaevich, c.t.s., docent, Abylkas Saginov Karaganda Technical University
e-mail: s.ahmediev@kstu.kz

Filippova Tatyana Silinyevna, c.t.s., professor, Abylkas Saginov Karaganda Technical University
e-mail: tsxfilippova@mail.ru

Oryntayeva Gulzhaukhar Zhunuskhanovna, senior lecturer, Abylkas Saginov Karaganda Technical University
e-mail: oryntaeva70@mail.ru

Tazhenova Gulzada Dauletkhanovna, c.t.s., docent, Abylkas Saginov Karaganda Technical University
e-mail: gulzada_2604@mail.ru